Chapter 1

Radiative Heat Transfer for Curvilinear Surfaces

Jose Maria Cabeza Lainez,
Jesus Alberto Pulido Arcas, Manuel-Viggo Castilla,
Carlos Rubio Bellido and
Juan Manuel Bonilla Martínez

Additional information is available at the end of the chapter

http://dx.doi.org/10.5772/59797

1. Introduction

Curved surfaces have not been thoroughly considered in radiative transfer analysis mainly due to the difficulties arising from the integration process and perhaps because of the lack of spatial vision of researchers. When dealing with them, application of the iterative method or direct calculation through integration does not provide with an exact solution, so that only approximate expressions or tables are given for a very limited number of forms [1]. In this way, a vast repertoire of significant shapes remains neglected and energy waste is evident. For this reason, further research on the matter, starting from a different approach was considered worth doing.

In previous researches from the authors, form factor calculation has been undertaken for several types of emitters. In all cases, geometric properties of those, revealed as the most powerful tool that shapes radiant interchange [3,4,5,6]. This included mainly rectangular shapes, plane forms and the volumes that can be composed with such primary geometries.

Following the same approach to radiative transfer through the basic understanding of the spatial and geometric properties of volumes, in this chapter new form factors derived from a combination of curvilinear surfaces are hereby presented. Starting from the properties of the sphere and with simple calculus, new laws are devised, which enable the authors to discover a set of configuration factors for caps and various segments of the sphere. The procedure is subsequently extended to the paraboloid, the ellipsoid or the cone, useful in issues such as rocket nozzle design and organic shapes contained in human physique. Appropriate combination of the said forms with truncated cones, produces highly articulate shapes, which

frequently occur in the technical domains but were not feasible for exact calculation during a number of years. The research is duly accomplished by presenting the equations needed to evaluate interreflections in curvilinear geometries. Thus, heat transfer simulation is enhanced by such results leading to create innovative software which has been expanded in turn by the authors.

2. Outline of the problem

The reciprocity principle enunciated by Lambert in 1760 and expressed in Eqn. (1), yields the following well-known integral equation (2) that acts as the theoretical basis for form factor calculation between two surfaces.

$$d\varnothing_{1\text{-}2} = (E_{b1} - E_{b2}) cos\theta_1 * cos\theta_2 * \frac{d A_1 * d A_2}{\pi * r^2} \tag{1}$$

$$\varnothing_{1\text{-}2} = (E_{b1} - E_{b2}) \int_{A_1} \int_{A_2} cos\theta_1 * cos\theta_2 * \frac{d A_1 * d A_2}{\pi * r^2} \tag{2}$$

Where the terms are depicted in Figure 1,

E_{bi}= radiant power emitted by the corresponding surface 1 or 2

A_i= area of surface, dA_i= differential of area

r = distance radiovector

θ_i =angle between radiovector at differential element *i* and the normal to the surface

The previous expression states that radiant interchange for every given form depends on its shape and its relative position in the three-dimensional space (Figure 1). From the times of Lambert to our days, researchers and scientists in the fields of geometric optics and radiative transfer have sought to provide solutions to the canonical equation (2) for a variety of forms [1]. This is no minor feat, since the said equation leads in most cases to a quadruple integration and the fourth degree primitive of even simple mathematical expressions often implies lengthy calculations.

Given the fact that this equation depends on geometric parameters, it is reasonable to think that there should be an easier way to approach the problem rather than dealing directly with the integral; also, with the aid of computer simulation, mathematical solutions of complex functions can be approached in a simple and friendly way. Curvilinear forms present some characteristics that make them suitable for a different treatment in terms of radiative transfer.

3. Form factors derived from the sphere

Starting from simple forms several form factors can be calculated without hardly any calculus; later, this logic can be applied to more complex configurations. Let us consider first the simplest

http://dx.doi.org/10.5772/59797

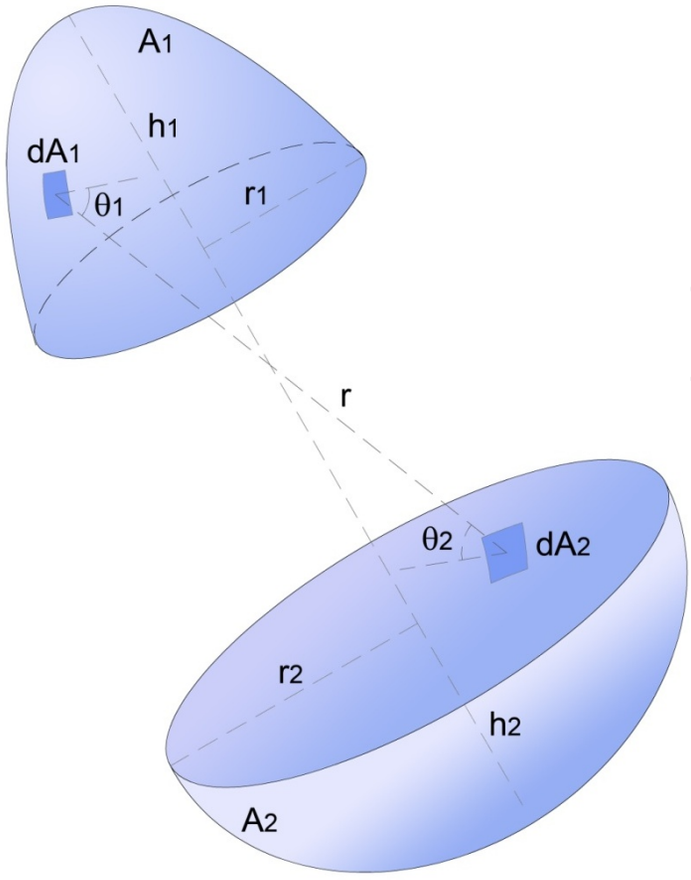

$$d\phi_{1\text{-}2} = (E_{b1}\text{-}E_{b2}) \cdot \cos\theta_1 \cdot \cos\theta_2 \cdot \frac{dA_1 \cdot dA_2}{\pi \cdot r^2}$$

Figure 1. The reciprocity principle and equation for arbitrary surfaces A_1 and A_2

form, a sphere that irradiates energy from its inner surface; the irradiated energy is entirely received by itself; so that, being the sphere surface 1, the only factor that has to be considered is:

$$F_{11}=1 \tag{3}$$

Bearing this in mind, in a similar surface, for instance a hemisphere, the form factor is accordingly F_{11}= ½. The configuration factor of a differential area to a disk of radius *r* under the center of the disk at precisely the distance *r*, provides a hint in that it is also ½ [2]. For a point of the hemisphere the factor required is ½.

Stimulated by this result, volumes composed of only two surfaces, one being planar and the other spherical, were analyzed. The first case was the spherical cap which is a generalization of the hemisphere.

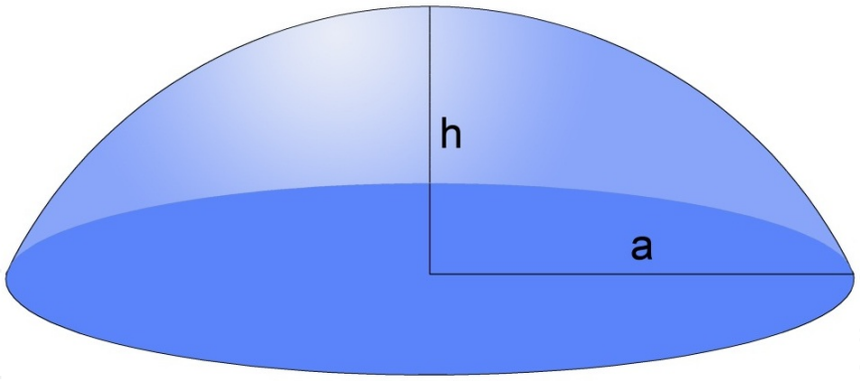

Figure 2. A spherical cap of height h and radius of the base a

Extending the reciprocity principle to a spherical cap (Fig. 2) of radius R (surface 1), and its entire base (surface 2) the factor was obtained from the relation $A_1 \cdot F_{12} = A_2 \cdot F_{21}$; since $F_{21}=1$, and there is no F_{22} for planar surfaces, $F_{12} = {A_2}/{A_1}$, in this particular case:

$$F_{12} = \frac{a^2}{a^2 + h^2} \tag{4}$$

$$F_{11} = \frac{h^2}{a^2 + h^2} = \frac{h}{2*R} \tag{5}$$

Two important laws are inferred from here, which have been defined as Cabeza-Lainez laws:

Cabeza-Lainez first law:

If a volume is encircled by two surfaces preseting one of them positive of thempositive curvature, and the second being planar, the exchange factor from the curved surfaceto the other equals the inverse ratio of areas of the aforementioned figures. The notion of positive curvature of the element is introduced to foresee stagnation of radiant flux.

Cabeza-Lainez second law:

Within a spherical surface the form factor of any given area over itself is precisely the fraction between that area and the sphere

The second law requires of more deduction as follows

Given that a spherical cap represents an Y^{th} fraction of the total area of the sphere of radius R, and recalling from trigonometry that,

$$(h^2 + a^2) = 2 \cdot R \cdot h \tag{6}$$

Thus,

http://dx.doi.org/10.5772/59797

$$Y \cdot (h^2 + a^2) = 4 \cdot R^2 \ (5);\ Y = 2 \cdot \frac{R}{h} \ (6);\ h = 2 \cdot \frac{R}{Y} \tag{7}$$

Consequently,

$$F_{11} = \frac{h}{2 \cdot R} = \frac{h^2 \cdot Y}{4 \cdot R^2} = \frac{1}{Y} \tag{8}$$

Cabeza-Lainez second law:

The configuration factor of an Y^{th} part of the sphere over itself is precisely the inverse of Y.

Thus, the assumption for the hemisphere is confirmed; in the quarter of sphere F_{11} has to be 1/4 and successively for every portion of the given sphere.

This law will hold true even if we are not dealing with spherical caps but for any fragment of the surface. Taking a critical look at the canonical equation (1) adapted to the sphere, it is logical to establish a relationship between r, $cos\theta$ and the radius R (Figure 3).

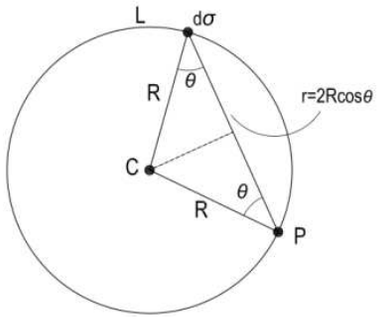

Figure 3. Differential surfaces in the sphere of centre C and luminance L used to find the radiative exchange

Substituting, these terms in the canonical equation (1):

$$\varnothing_{1\text{-}2} = \frac{E_{b1}}{4 \cdot \pi \cdot R^2} \int_{A_1} \int_{A_2} dA_1 \cdot dA_2 \tag{9}$$

$4\pi R^2$ is the total area of the sphere. Thus, the radiative flux transfer is dependent on the size of the surfaces but not on their position in the sphere and for given areas it is also a constant.

Trying to obtain $F_{11} = \frac{\varnothing_{11}}{E_{b1} \cdot A_1}$ from equation (7) gives the expression:

$$F_{11} = \frac{A_1}{4 \cdot \pi \cdot R^2} = \frac{1}{Y} \tag{10}$$

This means that spherical surfaces present these unique properties (Eqs. 3 and 8) which are crucial for our discussion crucial for our discussion.

Now Cabeza-Lainez laws can be applied to more complex volumes that involve portions of the sphere. Considering a sector of the sphere comprised between to semicircles forming an internal angle x from 0 to 180 degrees:

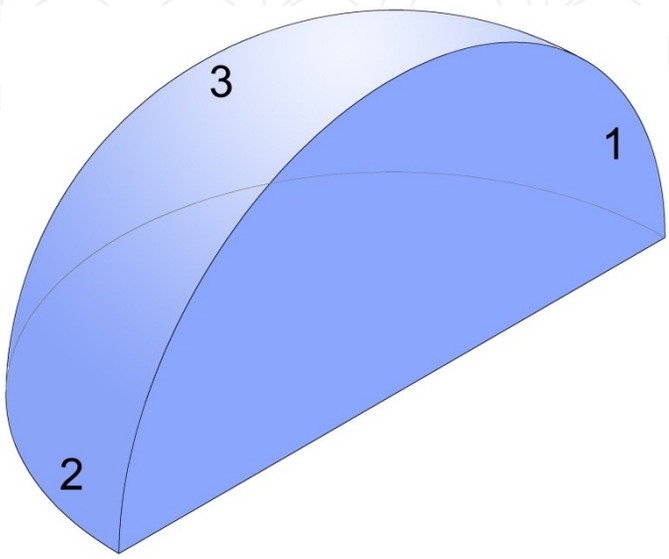

Figure 4. Denomination of surfaces in a sector of the sphere, 1 and 2 are planar semicircles, 3 is curved.

As has been discussed, the Y portion of the sphere is, in this case $^{1}/_{Y} = {}^{x}/_{360}$ and thus,

$$F_{33} = \frac{x}{360} \tag{11}$$

Accordingly,

$$F_{31} = F_{32} = \frac{1}{2} \cdot \left(1 - \frac{x}{360}\right) \tag{12}$$

And introducing the areas of the semicircles, $^{\pi R^2}/_{2}$

$$F_{13} = F_{23} = \frac{x}{90} \cdot \left(1 - \frac{x}{360}\right) \tag{13}$$

Following the discussion, these pair of semicircles can form any angle x between 0 and 360 degrees (Fig. 5). So that, the following equation, which has not been found expressed previously in the literature, is proposed in order to obtain the energy balance between the half disks, where x represents the value of their internal angle (Figure 5).

http://dx.doi.org/10.5772/59797

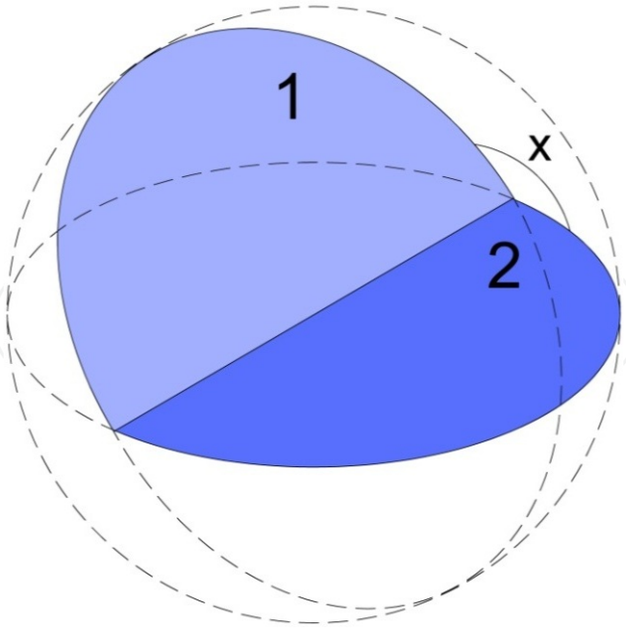

Figure 5. Two semicircles of the same radius R with a common edge forming an angle X

$$F_{12}=1 - \frac{x}{90} + \frac{x^2}{32400} \tag{14}$$

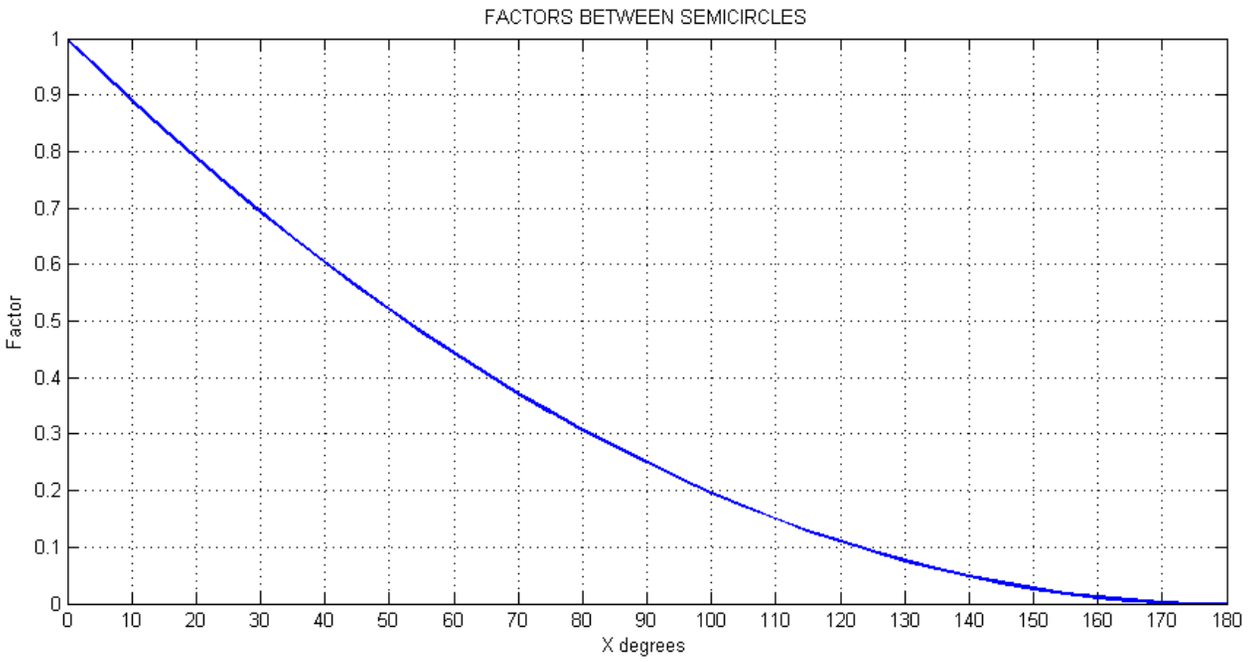

Figure 6. Radiative exchanges between two semicircles with a common edge and forming an internal angle x

The latter expression (Eq. 14) is a good indicator of the factor between two inclined and equal surfaces with a common edge. If they are not too dissimilar from the semicircle, a factor that is usually lengthy and cumbersome to calculate can be devised easily.

Let us now return to the first principle, the expression $\frac{h}{2R}$ (Eq. 5), applied to the spherical cap. Form factors between the contained surfaces are as follows:

$$F_{11} = \frac{h}{2 \cdot R} = \frac{h^2}{h^2 + a^2} \tag{15}$$

$$F_{12} = \frac{a^2}{h^2 + a^2} \tag{16}$$

$$F_{21} = 1 \tag{17}$$

If we introduce at this point the dimensionless parameter β, we can simplify equation 16 as,

$$\beta^2 = \frac{h^2}{a^2} \tag{18}$$

$$F_{12} = \frac{1}{\beta^2 + 1} \tag{19}$$

Since this principle is more general than the second one, we can extend it to non-spherical surfaces.

4. Application to common surfaces

4.1. Prolate semispheroid

Surface 1 is the spheroid and surface 2 is the circular disk that works as a base to the former, h>a.

Firstly the dimensionless parameter m is introduced:

$$m = \sqrt{1 - \frac{a^2}{h^2}} \tag{20}$$

By virtue of the first principle,

$$F_{12} = \frac{a*m}{a*m + h*\arcsin(m)} \tag{21}$$

http://dx.doi.org/10.5772/59797

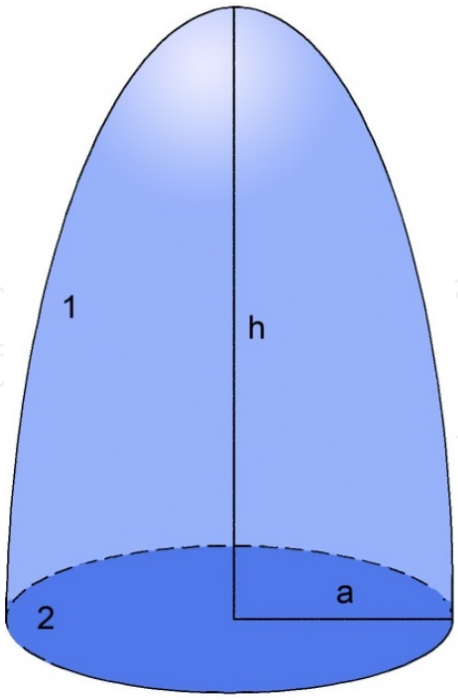

Figure 7. Prolate spheroid

$$F_{21}=1 \tag{22}$$

$$F_{11}=\frac{h*\arcsin(m)}{a*m+h*\arcsin(m)} \tag{23}$$

And making,

$$\beta^2=\frac{h^2}{a^2};\ m=\sqrt{1-\frac{1}{\beta^2}} \tag{24}$$

$$F_{12}=\frac{\sqrt{1-\frac{1}{\beta^2}}}{\sqrt{1-\frac{1}{\beta^2}}+\beta*\arcsin\left(\sqrt{1-\frac{1}{\beta^2}}\right)} \tag{25}$$

4.2. Oblate semiespheroid

Surface 1 is the spheroid and surface 2 is the circular disk that works as a base to the former, h<a

Denote the parameter m_1,

$$m_1=\sqrt{\frac{a^2}{h^2}-1} \tag{26}$$

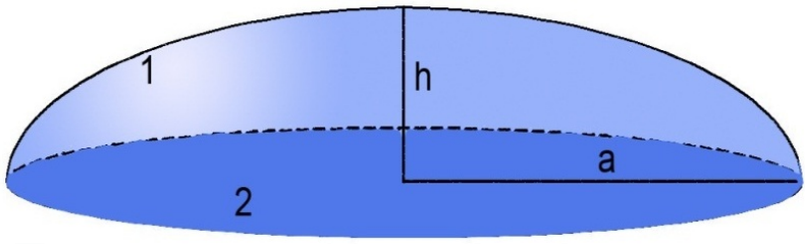

Figure 8. Oblate spheroid

$$F_{12} = \frac{a^{*}m_1}{a^{*}m_1 + h\,^{*}\text{arcsinh}\,(m_1)}\;;F_{21} = 1 \tag{27}$$

By the first principle and,

$$F_{11} = \frac{h\,^{*}\text{arcsinh}\,(m_1)}{a^{*}m_1 + h\,^{*}\text{arcsinh}\,(m_1)} \tag{28}$$

With the same procedure as before to make the expression dimensionless

$$m_1 = \sqrt{\frac{1}{\beta^{2}} - 1} \tag{29}$$

$$F_{12} = \frac{m_1}{m_1 + \beta^{*}\text{arcsinh}\,(m_1)} \tag{30}$$

4.3. Paraboloid of revolution

Surface 1 is the paraboloid and surface 2 is the circular disk that works as a base to the former

$$F_{12} = \frac{6^{*}a^{*}h^{\,2}}{\left[\left(a^{2} + 4^{*}h^{\,2}\right)^{3/2} - a^{3}\right]}\;;F_{21} = 1 \tag{31}$$

$$F_{11} = 1 - \frac{6^{*}a^{*}h^{\,2}}{\left[\left(a^{2} + 4^{*}h^{\,2}\right)^{3/2} - a^{3}\right]} \tag{32}$$

$$\beta = \frac{h}{a}\;;F_{12} = \frac{6^{*}\beta^{2}}{\left[\left(1 + 4^{*}\beta^{2}\right)^{3/2} - 1\right]} \tag{33}$$

4.4. Right cone

1 is the surface of the cone and 2 is the circular base

$$F_{12} = \frac{a}{\sqrt{a^{2} + h^{\,2}}}\;;F_{21} = 1 \tag{34}$$

http://dx.doi.org/10.5772/59797

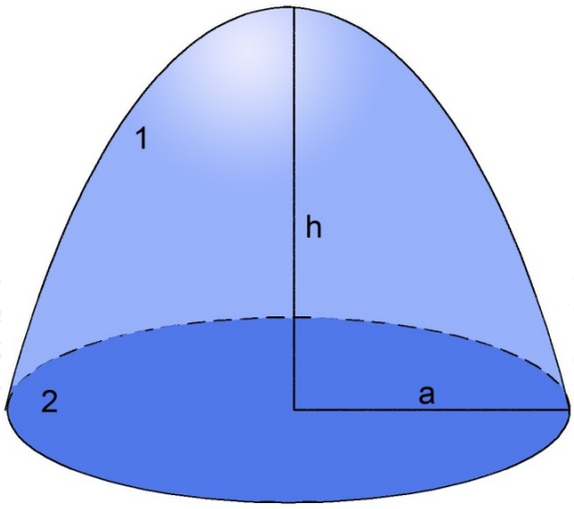

Figure 9. Paraboloid of revolution

$$F_{11}=1-\frac{a}{\sqrt{a^2+h^2}} \tag{35}$$

Introducing the parameter β,

$$F_{12}=\frac{1}{\sqrt{1+\beta^2}} \tag{36}$$

It is possible to compare the performance in terms of F_{12}, of all the figures found up to now, where the cone shows better performance followed by the paraboloid.

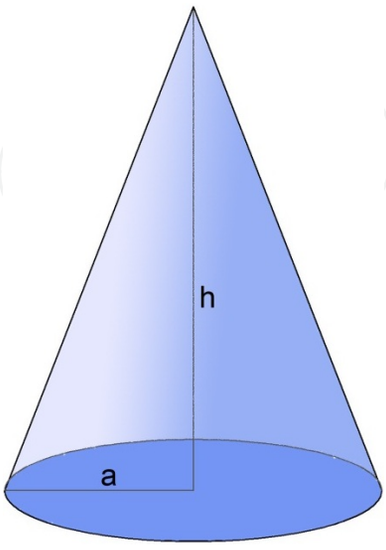

Figure 10. Cone

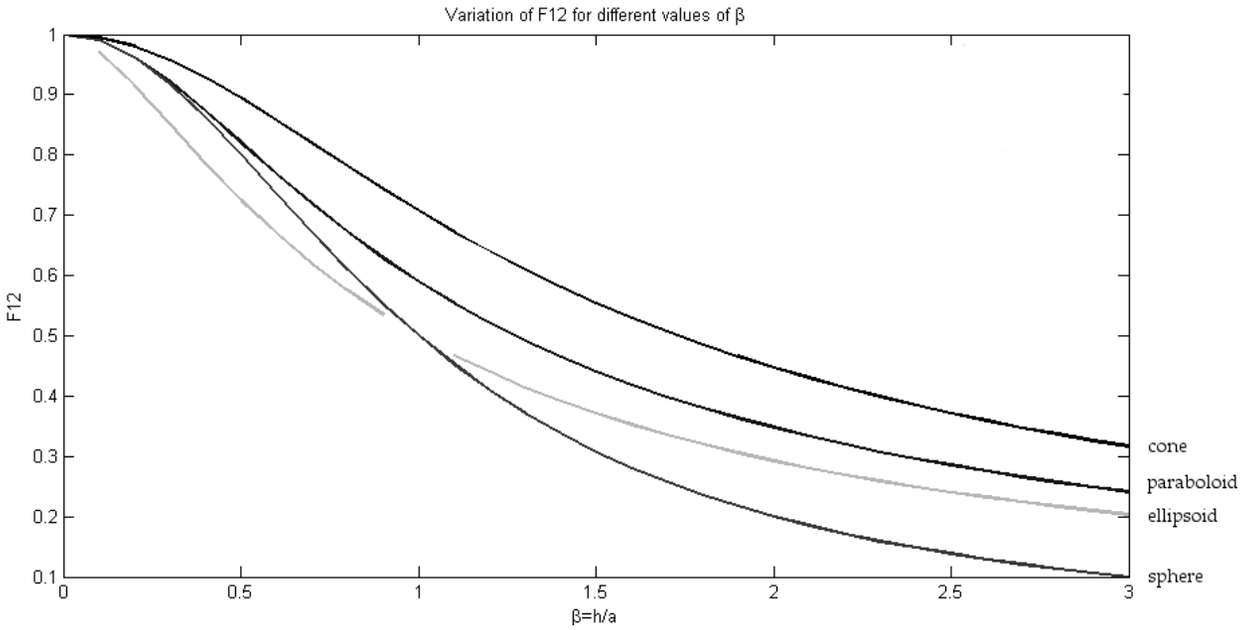

Figure 11. Comparison of form factors for different shapes

4.5. Ellipsoid

In this case, 1 is the surface of the ellipsoid and 2 is the elliptic base; y is a parameter equal to 1.6. The example shows that the first principle is not limited to surfaces of revolution.

$$F_{12}=\frac{a*b*\sqrt[y]{3}}{2*\sqrt[y]{a^{y}*b^{y}+a^{y}*h^{y}++b^{y}*h^{y}}};F_{21}=1 \tag{37}$$

$$F_{11}=1-\frac{a*b*\sqrt[y]{3}}{2*\sqrt[y]{a^{y}*b^{y}+a^{y}*h^{y}++b^{y}*h^{y}}} \tag{38}$$

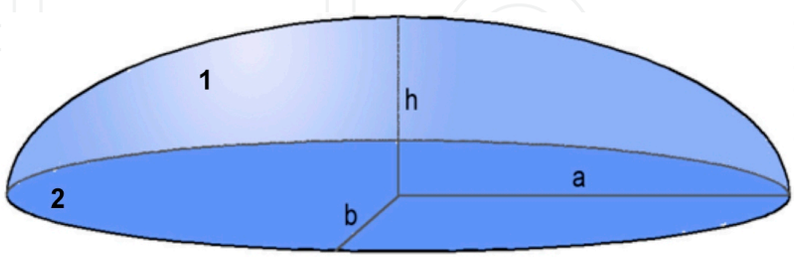

Figure 12. Ellipsoid

As the area of the ellipsoid is not exact, we can expect errors on the range of 1% depending on the values of a, b and h.

This principle can be also used in other surfaces, for example, for two complementary caps within the sphere of radius r,

http://dx.doi.org/10.5772/59797

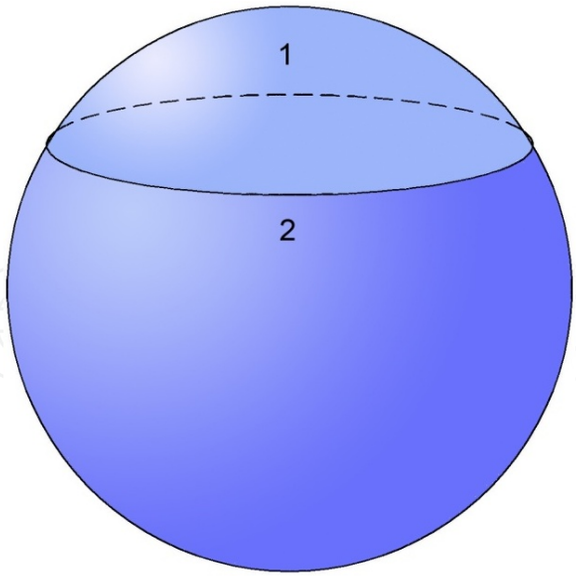

Figure 13. Sphere divided in two caps of diverse heights

As an immediate consequence of Cabeza-Lainez laws, r being the radius of the inner circle and h the respective heights of the caps,

$$F_{11}=F_{21}=\frac{h_1^2}{h_1^2+r^2}=\frac{r^2}{h_2^2+r^2}=\frac{h_1*h_2}{h_2^2+r^2}=\frac{h_1^2+r^2}{(h_1+h_1)^2}=\frac{h_1}{(h_1+h_2)}=\frac{h_1}{2*R} \tag{39}$$

$$F_{22}=F_{12}=\frac{h_2^2}{h_2^2+r^2}=\frac{r^2}{h_1^2+r^2}=\frac{h_1*h_2}{h_1^2+r^2}=\frac{h_2}{(h_1+h_2)} \tag{40}$$

If now the caps within the same sphere are of any size and arbitrary position,

In this case by virtue of Cabeza-Lainez Law,

$$F_{11}=\frac{h_1^2}{h_1^2+a^2};\ F_{22}=\frac{h_2^2}{h_2^2+a_2^2} \tag{41}$$

And now we need to apply the canonical equation 9 again, substituting the respective areas of the caps; $A_1=2.\pi.R.h_1$. ; $A_2=2.\pi.R.h_2$

$$\varnothing_{1\text{-}2}=\frac{E_{b1}}{4*\pi*R^2}\int_{A_1}\int_{A_2} dA_1*dA_2 \tag{42}$$

$$F_{12}=\frac{h_1*h_2}{h_1^2+a^2};\ F_{21}=\frac{h_1*h_2}{h_2^2+a_2^2} \tag{43}$$

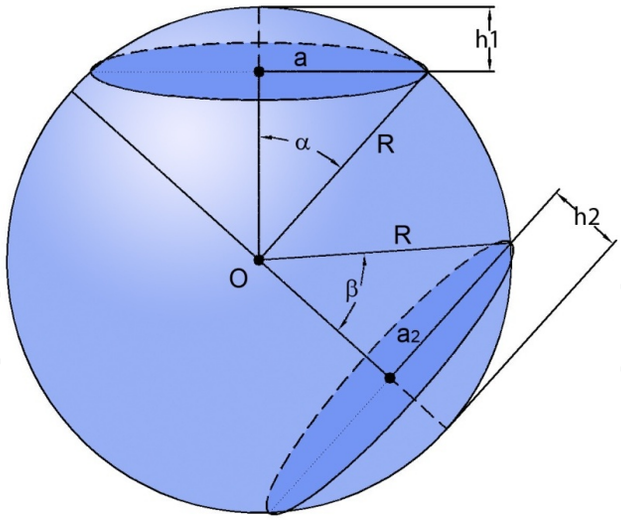

Figure 14. Two caps of arbitrary size

In the special situation that the caps are parallel, which equates a truncated cone, the flux would be $E_{b1}.\pi.h_1.h_2$ and the fraction of energy from disk 1 to disk 2 (or their surrounding caps), equates $h_1{*}h_2/a^2$ or $h_1{*}h_2/a_2^2$. In the case that the bases are of equal radius a, h1=h2=h. If the perpendicular distance between the disks, called 2b, is known (Figure 15), the height of the cap would be,

$$h = \sqrt{a^2 + b^2} - b \tag{44}$$

Thus, the fraction is obtained as,

$$F_{12} = F_{21} = \frac{a^2 + 2{*}b^2 - 2{*}b{*}\sqrt{a^2 + b^2}}{a^2} \tag{45}$$

By virtue of equation 45 it is feasible to address radiative transfer in several figures composed of three surfaces and limited by parallel disks like truncate paraboloids, caps and especially cylinders. Appropriate equations can be easily formed in which only two values need to be found. To the circles in the extremes of the cylinder a spherical cap could be connected (fig. 16) and the radiative transfer would not be altered significantly since we have previously described the performance of caps limited by circles. In the particular case that the cap is a hemisphere, the factor already determined ought to be multiplied by 0.5 and subsequently for different curvatures, bearing in mind that the unity is the circle and null would imply a "theoretical" whole sphere [1]

1 Note that values under 0.5 can also be found for this relationship in a sort of globular cap with an area bigger than the hemisphere.

http://dx.doi.org/10.5772/59797

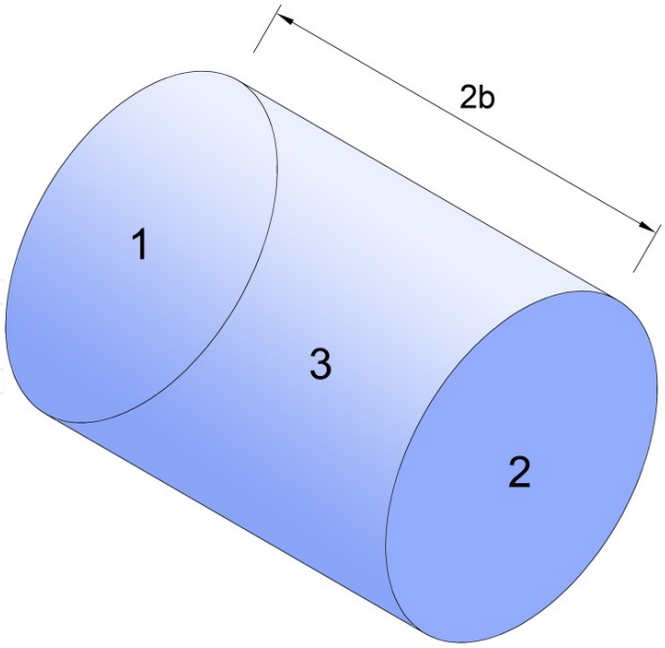

Figure 15. Surfaces defined by a cylindrical volume used to find the radiative transfer

The space of figure 16 has been used throughout the history of buildings in cathedrals, opera houses, museums and assembly halls. If both extremes are curved, such shape is still found at bunkers, water tanks and pressure vessels of power reactors.

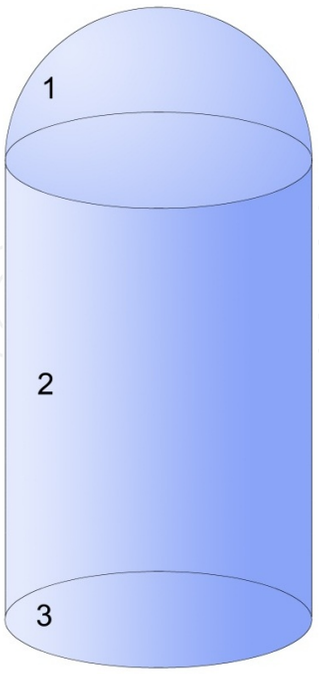

Figure 16. Volume composed of a cylinder and a spherical cap used to find the radiative transfer among those surfaces

4.6. Two opposed spherical caps with a common axis

In order to calculate the radiative exchanges in this relatively complex figure, we need to determine beforehand the following nine geometric parameters that depend on the geometric variables shown in Figure 17.

$$z = \frac{r_1^2 - r_2^2}{4*b};\ R = \sqrt{(z+b)^2 + r_2^2} \tag{46}$$

$$l = \sqrt{(r_1 - r_2)^2 + 4*b^2} \tag{47}$$

$$Q = R^2 - z^2 + b^2 - 2*R*b \tag{48}$$

$$Q_1 = r_1^2 - Q\ ;\ Q_2 = r_2^2 - Q \tag{49}$$

$$D_1 = h_1^2 + r_1^2 \tag{50}$$

$$D_2 = h_2^2 + r_2^2 \tag{51}$$

$$D_3 = l*(r_1 + r_2) \tag{52}$$

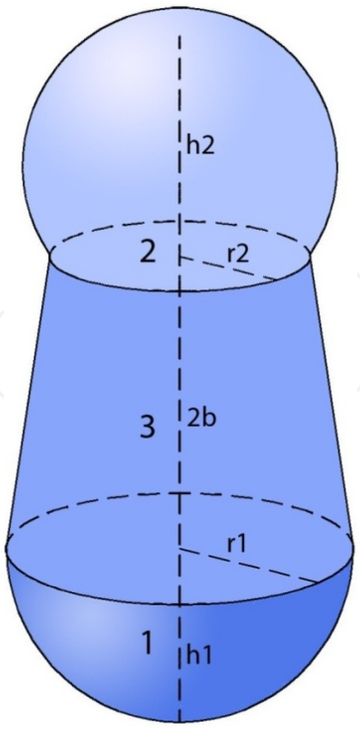

Figure 17. Volume composed by spherical cap, truncated cone and hemispheroid.

http://dx.doi.org/10.5772/59797

And then we would obtain the corresponding nine form factors involved,

$$F_{11}=\frac{h_1^2}{D_1};\ F_{12}=\frac{Q}{D_1};\ F_{13}=\frac{Q_1}{D_1} \tag{53}$$

$$F_{22}=\frac{h_2^2}{D_2};\ F_{21}=\frac{Q}{D_2};\ F_{23}=\frac{Q_2}{D_2} \tag{54}$$

$$F_{31}=\frac{Q_1}{D_3};\ F_{32}=\frac{Q_2}{D_3};\ F_{33}=1-\frac{Q_1+Q_2}{D_3} \tag{55}$$

In this simple way the problem is completely solved

4.7. Straight cone

This is a limit case of the previous discussion.

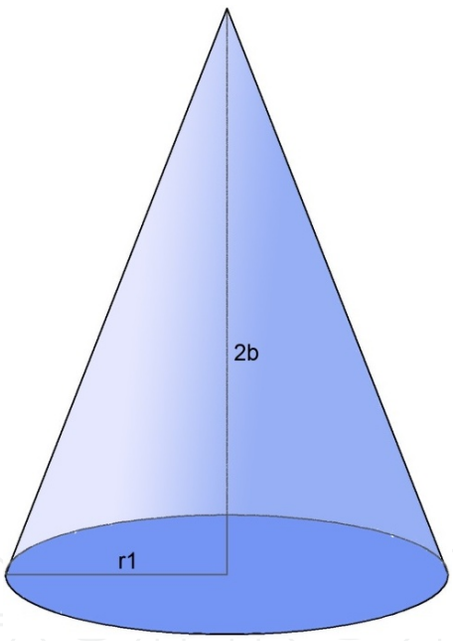

Figure 18. Right cone with a circular base

As the former also includes the cone, by making $r_0=0$ and $h_1=h_2=0$, $Q_2=0$, $z=\frac{r_1^2}{4b}$, $R=z+b$, $Q=0$, $Q_1=0$, $Q_2=0$

$$l=\sqrt{r_1^2+4*b^2} \tag{56}$$

If $D_1=r_1^2$, $D_2=0$ then

$$D_3 = \sqrt{r_1^2 + 4*b^2} \tag{57}$$

Only three factors remain,

$$F_{11} = 1 \tag{58}$$

$$F_{31} = \frac{r_1}{\sqrt{r_1^2 + 4*b^2}} \tag{59}$$

$$F_{33} = 1 - \frac{r_1}{\sqrt{r_1^2 + 4*b^2}} \tag{60}$$

F_{31} is obviously the ratio of areas of the cone to its base which proves that the equation is true, by virtue of Cabeza-Lainez Law.

4.8. Paraboloid, truncated cone and spheroid

If for instance, the upper extreme of the volume is a paraboloid and the lower surface is an oblate ellipsoid (Figure 19), we can still maintain the same factors with the following simple adaptations,

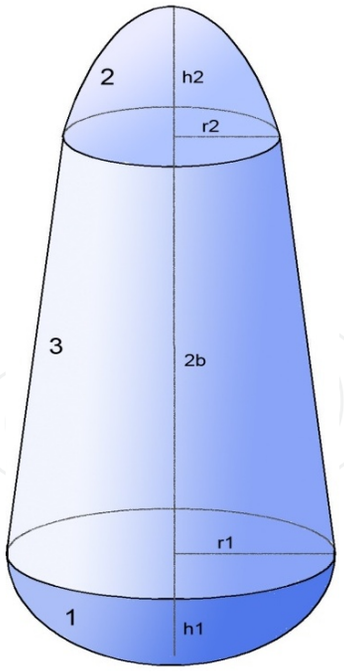

Figure 19. Volume composed by a paraboloid, a truncated cone and a spheroid.

$$F_{22} = 1 - \frac{6*r_2*h_2^2}{\left[\left(r_2^2 + 4*h_2^2\right)^{3/2} - r_2^3\right]} \tag{61}$$

as in the paraboloid alone

$$F_{21} = \frac{6*h_2^{2}*Q}{r_2*\left[\left(r_2^2 + 4*h_2^{2}\right)^{3/2} - r_2^{3}\right]} \tag{62}$$

$$F_{23} = \frac{6*h_2^{2}*\left(r_2^2 - Q\right)}{r_2*\left[\left(r_2^2 + 4*h_2^{2}\right)^{3/2} - a_2^{3}\right]} \tag{63}$$

$$F_{11} = \frac{h_1*\text{arcsinh}\,(m_1)}{r*m_1 + h_1*\text{arcsinh}\,(m_1)} \tag{64}$$

as it were in the oblate elipsoid alone

$$m_1 \text{ is now} = \sqrt{\frac{r_1^2}{h_1^2} - 1} \tag{65}$$

$$F_{12} = \frac{m_1*Q}{r_1*(r*m_1 + h_1*\text{arcsinh}\,(m_1))} \tag{66}$$

$$F_{13} = \frac{m_1*\left(r_1^2 - Q\right)}{r_1*(r_1*m_1 + h_1*\text{arcsinh}\,(m_1))} \tag{67}$$

F_{31}, F_{32} and F_{33} have the same values as before as these correspond to the truncated cone and bear only nominal relation with the surfaces of the extremes,

$$F_{31} = \frac{Q_1}{D_3} \tag{68}$$

$$F_{32} = \frac{Q_2}{D_3} \tag{69}$$

$$F_{33} = 1 - \frac{Q_{1+}Q_2}{D_3} \tag{70}$$

Similar results will be obtained when the truncate is a paraboloid instead of a cone as it is the case in rocket nozzles.

4.9. Summary of the findings

All the aforementioned form factors have been obtained by logical deduction. In order to provide researchers and designers with all this factors in a compact format, the following table is presented, which comprises all the volume configurations presented in this chapter.

F_{21} is always the unit as shown by first law

SURF.	Area of the revolution surface	$F_{1\rightarrow 1}$	$F_{1\rightarrow 2}$
Prolate semi-spheroid with circular base	$2\pi a^2 \frac{arcsen(m)\cdot(h+am)}{a\cdot m}$ $m=\sqrt{1-{a^2}/{h^2}}$	$\frac{h*\arcsin(m)}{a*m+h*\arcsin(m)}$	$\frac{a*m}{a*m+h*\arcsin(m)}$
Oblate semi-spheroid with elliptic base	$2\pi a^2 \frac{arcsenh(m)\cdot(h+am)}{a\cdot m}$ $m=\sqrt{{a^2}/{h^2}-1}$	$\frac{h*\arcsin(m_1)}{a*m_1+h*\arcsin(m_1)}$	$\frac{a*m_1}{a*m_1+h*\arcsin(m_1)}$
Revolution paraboloid with circular base	$\pi\frac{\sqrt[3]{a^2+4h^2}^2-a^3}{6a^3h^2}$	$1-\frac{6*a*h^2}{\left[(a^2+4*h^2)^{3/2}-a^3\right]}$	$\frac{6*a*h^2}{\left[(a^2+4*h^2)^{3/2}-a^3\right]}$
Straight cone with circular base	$\pi a\sqrt{a^2+h^2}$	$1-\frac{a}{\sqrt{a^2+h^2}}$	$\frac{a}{\sqrt{a^2+h^2}}$
Revolution Ellipsoid	$4\pi\left(\frac{a^y b^y+a^y h^y+b^y h^y}{3}\right)^{1/y}$ $y={8}/{5}$	$1-\frac{(ab\sqrt[y]{3})/2}{\sqrt[y]{a^y b^y+a^y h^y++b^y h^y}}$	$\frac{(ab\sqrt[y]{3})/2}{\sqrt[y]{a^y b^y+a^y h^y++b^y h^y}}$

Table 1. Resume of form factors for curved surfaces.

5. Interreflections amongst surfaces in a closed volume

Until this point the discussion has dealt with primary transmission of energy but, in a closed space, if the surfaces have some degree of reflectivity a significant part of the flux would be re-irradiated and the concepts of emitters and receivers entwine.

Under such circumstance, the global balance of radiant power can be found through expression 71,

$$E_{tot}=E_{dir}+E_{ref} \tag{71}$$

E_{dir} is defined as the direct power received while E_{ref} stands for the reflected energy. The two quantities added yield the global balance of radiant energy E_{tot}. If the problem entails several surfaces, expression 71 is expanded for an array of equations. To resolve it, we define beforehand the matrices F_d and F_r, whose elements are described as follows in a three-dimensional fashion, (see figure 16):

$$F_d=\begin{pmatrix} F_{11}*\rho_1 & F_{12}*\rho_2 & F_{13}*\rho_3 \\ F_{21}*\rho_1 & F_{22}*\rho_2 & F_{23}*\rho_3 \\ F_{31}*\rho_1 & F_{32}*\rho_2 & F_{33}*\rho_3 \end{pmatrix} \tag{72}$$

http://dx.doi.org/10.5772/59797

$$F_r = \begin{pmatrix} 1 & -F_{12}*\rho_2 & -F_{13}*\rho_3 \\ -F_{21}*\rho_1 & 1 & -F_{23}*\rho_3 \\ -F_{31}*\rho_1 & -F_{32}*\rho_2 & 1 \end{pmatrix} \quad (73)$$

Each term in equations 72 and 73 is presented in the form F_{ij} (F_{11}, F_{12}...). This stands for the configuration factors already found, from one of the surfaces *i* to another adjacent surface *j*. The term ϱ_i is defined as the reflective quotient which corresponds to a given surface *i*.

A detailed explanation for the phenomenon is given in [3]. Formerly, as volumes considered were limited by planes, all the elements in the diagonal of matrix F_d were equal to zero and we could not deal with the problem while, for curved surfaces, the values of the diagonal are different from null and need to be calculated with the expressions hereby presented.

Once the value of these matrices is obtained, it is easy to establish the following relationship between direct and reflected radiation:

$$F_r * E_{ref} = F_d * E_{dir} \quad (74)$$

$$F_{rd} = F_r^{-1} * F_d \quad (75)$$

$$E_{ref} = F_{rd} * E_{dir} \quad (76)$$

As the value of reflected radiation is known, the problem is solved. However, we have to bear in mind that the number of surfaces should be augmented depending on the dimensions of the case study. The procedure for interreflection can be considered iterative depending on the accuracy that is required for a particular problem [3].

The simplest case of repeated reflections appears in the sphere and is wont to be employed in lieu of the former calculations with matrices.From expression 9 and successive, it was deducted that energy impinging on a point of the sphere from an emitter contained in the same surface equates the quotient between the area of the emitting surface and the total area 4 πR2, and it can be expressed under the form W/A.

After a relevant number of reflections, the total power distributed over the sphere is defined by:

$$E_{ref} = E * \frac{W}{A} * \left(\rho + \rho^2 + \ldots \rho^n\right) \quad (77)$$

As,

$$\lim_{n \to \infty} \left(\frac{\rho^{n+1} - 1}{\rho - 1} - 1\right) = \frac{\rho}{1 - \rho} \quad (78)$$

$$E_{ref} = E * \frac{W}{A} * \left(\frac{\rho}{1 - \rho} \right) \tag{79}$$

In the precedent discussion ϱ includes the mean of all reflection quotients ϱ_i inside the sphere, while E represents the direct power exiting from the source. Such expression would be technically applicable to all kinds of surfaces, but its accuracy dwindles when the actual volume is not akin to a sphere. If such is the case, equation 79 would be less acceptable.

Since the reflectivity of the internal surfaces can be changed on demand, the way to treat glazed elements or voids is to assign them a high absorption coefficient to ensure that those elements play a limited role in the global energy balance.

6. Conclusions

An ever-increasing number of configuration factors for curved geometries, has been deducted. The authors have extracted the former in total conformity with the procedures of optical mechanics and thus the new factors can be termed as exact in contrast with other random or discretized methods.

This represents an indubitable advance of knowledge for radiative heat transfer that is already being implemented in computer models. However, the details of the simulation procedures are not discussed in this chapter in the credence that other scientists will arrive with perfect ease to the required algorithms.

Thus, this new form factors have been programmed in computer algorithms, creating a powerful tool that is able to enrich the repertoire of forms and spaces suitable for simulation. This procedure will benefit energy-conscious engineering and architecture, as has been demonstrated by the authors in previous publications [7, 8,9,10] Indeed, the prototypes based on the science of heat transfer are sure to progress in their accuracy and sophistication. Radiative devices and fixtures can be conceived departing from the findings exposed previously on a more scientific basis and this will be beneficial to expand the innumerable boons of solar radiation.

Contemplating the ruins of the colossal statues of Ramses in Egypt, Shelley once wrote:

My name is Ozymandias, King of Kings, Look on my works ye Mighty And Despair

Acknowledgements

Jose Cabeza would like to thank his family in Japan and Spain for failing to understand his work.

http://dx.doi.org/10.5772/59797

Author details

Jose Maria Cabeza Lainez[1,2*], Jesus Alberto Pulido Arcas[3], Manuel-Viggo Castilla[4], Carlos Rubio Bellido[4] and Juan Manuel Bonilla Martínez[5]

*Address all correspondence to: crowley@us.es

1 Universidad de Sevilla, Spain

2 Hokkaido University, Japan

3 Canon Foundation Fellow. University of Shiga Prefecture, Japan

4 Universidad de Sevilla, Spain

5 Universidad Politécnica de Cataluña, Spain

References

[1] John R. Howell, A Catalogue of Radiation Heat Transfer Configuration Factors. 3rd ed., 2010. On-line version available at: http://www.engr.uky.edu/rtl/ Catalog/.

[2] Buschman, Albert Jr. and Pittman, Claud M., 1961, "Configuration factors for exchange of radiant energy between axisymmetrical sections of cylinders, cones, and hemispheres and their bases," NASA TN D-944.

[3] Cabeza-Lainez Jose M. Solar Radiation In buildings. Performance and Simulation procedures. InTech. 2012.

[4] Cabeza Lainez Jose M. New Configuration Factors for Curved Surfaces. Journal of Quantitative Spectroscopy and Radiative Transfer (JQSRT). Vol. 117. March 2013.

[5] Cabeza Lainez Jose M. New configuration factor between a circle, a sphere and a differential area at random positions. Journal of Quantitative Spectroscopy and Radiative Transfer (JQSRT). Vol. 133. November 2013

[6] Cabeza Lainez Jose M. Fundamentals of Luminous Radiative Transfer. Netbiblo. 256 pg. December 2010.

[7] Cabeza Lainez Jose M, Jimenez Verdejo Juan R. The Japanese Experience of Environmental Architecture through the Works of Bruno Taut and Antonin Raymond. Journal of Asian Architecture and Building Engineering (JAABE). Pp. 33-40. May 2007.

[8] Cabeza-Lainez Jose M. Lighting Features in Japanese Traditional Architecture. In Lessons from Vernacular Architecture. Earthscan Routledge. 215 pp. August 2013.

[9] Cabeza Lainez Jose M. The quest for light in Indian Architectural Heritage. Journal of Asian Architecture and Building Engineering. Pp. 39-46. May 2008.

[10] Cabeza Lainez Jose M, Jimenez Verdejo Juan R. The Key-role of Eladio Dieste, Spain and the Americas in the Evolution from Brickwork to Architectural Form. Journal of Asian Architecture and Building Engineering (JAABE). Pp. 355-362. November 2009.

IntechOpen